

# Investigation of the $\gamma$ -decay behavior of $^{52}\text{Cr}$ with the $\gamma^3$ setup at HI $\gamma$ S

J. Wilhelmy<sup>1</sup>, P. Erbacher<sup>2</sup>, U. Gayer<sup>3</sup>, J. Isaak<sup>4</sup>, B. Löher<sup>5</sup>,  
M. Müscher<sup>1</sup>, S.G. Pickstone<sup>1</sup>, N. Pietralla<sup>3</sup>, P. Ries<sup>3</sup>, C. Romig<sup>3</sup>,  
D. Savran<sup>5</sup>, M. Spieker<sup>1</sup>, W. Tornow<sup>6</sup>, V. Werner<sup>3</sup>, A. Zilges<sup>1</sup> and  
M. Zweidinger<sup>3</sup>

<sup>1</sup> Institute for Nuclear Physics, University of Cologne, Germany

<sup>2</sup> Institute for Applied Physics, University of Frankfurt, Germany

<sup>3</sup> Institute for Nuclear Physics, TU Darmstadt, Germany

<sup>4</sup> Research Center for Nuclear Physics, Osaka, Japan

<sup>5</sup> Research Division, GSI, Darmstadt, Germany

<sup>6</sup> Department of Physics, Duke University, USA

E-mail: wilhelmy@ikp.uni-koeln.de

**Abstract.** The  $\gamma$ -ray strength function is an important input parameter for the calculation of nucleosynthesis processes. To study the dipole response in more detail, the  $\gamma$ -decay behavior of the *fp* shell nucleus  $^{52}\text{Cr}$  was investigated with the high-efficiency  $\gamma^3$  setup at the High Intensity  $\gamma$ -ray Source facility at TUNL in Durham, USA. The highly intense quasi mono-energetic  $\gamma$ -ray beam allows for excitations selective in multipolarity ( $J=1$  and  $J=2$ ) and energy. The  $\gamma^3$  setup is a multi-detector array consisting of HPGe and LaBr<sub>3</sub> detectors with high efficiency and enables the measurement of  $\gamma$ - $\gamma$  coincidences. Experimental results of  $^{52}\text{Cr}$  will be presented and discussed in this contribution.

## 1. Introduction

The  $\gamma$ -ray strength function (SF) is an important input parameter for theoretical calculations of nucleosynthesis processes under extreme conditions, e.g., supernovae explosions or binary star mergers. One relevant physics setting is the photon bath in which the seed nuclei undergo radiative capture reactions and photoabsorption reactions. An increase of the SF at lower energies (upbend) has been claimed for several nuclei in different mass regions and it is still under debate if this is a general phenomenon [1, 2, 3, 4, 5, 6, 7, 8, 9, 10]. The SF is dominated by E1, M1, and E2 strength. With parameters constrained by the isovector giant dipole resonance (IVGDR), the E1 part of the SF is in first order well described by the Generalized Lorentzian Model (GLO) [11]. However, at around 5 to 8 MeV, additional E1 strength on top of the low-energy tail of the IVGDR is observed in nuclei with excess neutrons [12]. This resonance-like structure, also denoted as Pygmy Dipole Resonance (PDR), is studied with various probes [12]. The Nuclear Resonance Fluorescence method (NRF) is very powerful to selectively excite dipole states in an environment of states with different spins. Using linearly polarized  $\gamma$ -ray beams, parity quantum numbers can be determined [13] with the  $\gamma^3$  coincidence setup at HI $\gamma$ S. For several medium to heavy-mass nuclei reduced transition strengths were investigated in  $(\gamma, \gamma')$ -



experiments. Low-lying dipole strength was also studied recently in the  $A \approx 50$  nuclear mass region in some Ca isotopes [14, 15, 16], Ni isotopes [17, 18], and in the nuclide  $^{52}\text{Cr}$  [19]. At higher energies the M1 Gamow-Teller giant resonance is observed, e.g., at around 8 to 9 MeV for nuclei in this mass region [20]. These 1p-1h excitations across closed major shells correspond predominately to the  $1f_{7/2} \rightarrow 1f_{5/2}$  spin-flip excitation in this mass region. The  $B(\text{M1})$  strength was investigated for different neighboring isotopes of  $^{52}\text{Cr}$ , e.g., by  $(\gamma, \gamma')$ -experiments on  $^{50}\text{Cr}$ ,  $^{56}\text{Fe}$  and  $^{60}\text{Ni}$ , as well by  $(e, e')$ -experiments for the  $N = 28$  isotones  $^{50}\text{Ti}$ ,  $^{52}\text{Cr}$  and  $^{54}\text{Fe}$  [21, 22, 23, 24]. For the  $N = 28$  nuclei it was shown that the magnetic dipole strength significantly influences, e.g., neutrino-nucleus cross sections [25].

## 2. Experimental setup

### 2.1. The High Intensity Gamma-ray Source

At the High Intensity Gamma-ray Source (HI $\gamma$ S), almost fully polarized  $\gamma$ -ray beams are generated by Laser Compton backscattering (LCB) inside the Free-electron Laser (FEL) optical cavity [26]. In this optical cavity, the eV-photons are generated by magnetic undulators and reflected by optical mirrors. The next incoming electron bunch collides with the low-energy photons and the relativistic electrons boost them to MeV-energies. Because Compton scattering conserves the polarization of the primary laser photons, the resulting  $\gamma$ -ray beam is almost fully polarized [27]. The resulting  $\gamma$ -beam energy profile is quasi-monoenergetic. After the scattering process the  $\gamma$ -ray beam is collimated and provided for experiments at the  $\gamma^3$  setup. For  $^{52}\text{Cr}$  twelve energy settings were measured for about 5 hours each.

### 2.2. The $\gamma^3$ setup

The high efficiency  $\gamma$ - $\gamma$  coincidence setup ( $\gamma^3$  setup) is a multi-detector array. Highly efficient  $\text{LaBr}_3$  detectors and HPGe detectors with high energy resolution can be combined depending on the demands of an individual experiment [28]. In the present experiment, four  $\text{LaBr}_3$  detectors were combined with four HPGe detectors to take advantage of both, high efficiency and high energy resolution. Two HPGe detectors and two  $\text{LaBr}_3$  detectors were placed at  $\Theta = 90^\circ$  with respect to the beam axis. This allows a direct measurement of parity quantum numbers, because of the angular distribution of the E1 and M1 transitions. Additionally, two HPGe and two  $\text{LaBr}$  detectors were placed under backward angles.

## 3. Analysis

### 3.1. Parity quantum numbers

For the determination of parity quantum numbers an experimental asymmetry  $\epsilon$  is defined [13, 29]:

$$\epsilon = \frac{N_{\parallel} - N_{\perp}}{N_{\parallel} + N_{\perp}} \quad (1)$$

$N_{\parallel}$  and  $N_{\perp}$  denote the  $\gamma$ -ray intensities parallel and perpendicular to the plane of polarization, respectively, corrected by the detector efficiencies. The detector efficiencies were determined with standard calibration sources ( $^{56}\text{Co}$  and  $^{226}\text{Ra}$ ) up to 3 MeV. Additionally, for higher energies, Monte-Carlo simulations using GEANT4 were performed. Because of the opening angle of the detectors, the experimental asymmetry is not -1 (negative parity quantum numbers) or +1 (positive parity quantum numbers), but around  $\pm 0.9$ . This still allows a clear assignment of parity quantum numbers. For  $^{52}\text{Cr}$  the parity quantum numbers of 41 levels were determined.

### 3.2. $\gamma$ -decay behavior

The  $\gamma$ -decay behavior was investigated via HPGe singles spectra and projected HPGe spectra from  $\text{LaBr}$ -HPGe coincidence data. Because of the quasi-monoenergetic  $\gamma$ -ray beam elastic

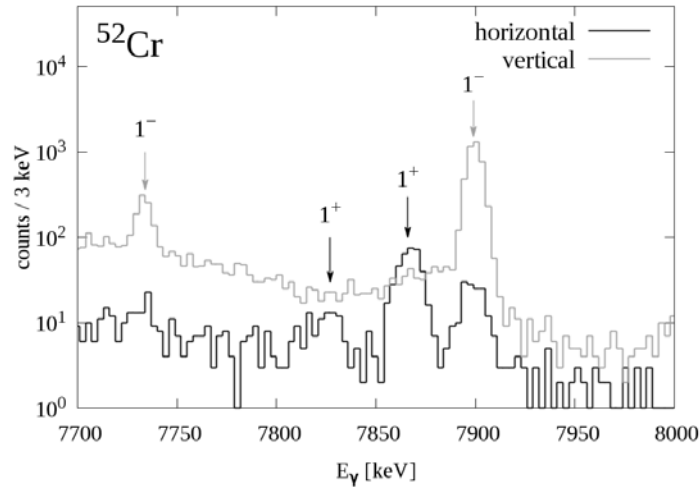


**Figure 1.** Two HPGe detector spectra in plane (black) and out of plane (grey) are shown. The  $\gamma$ -ray beam energy was 7.9 MeV

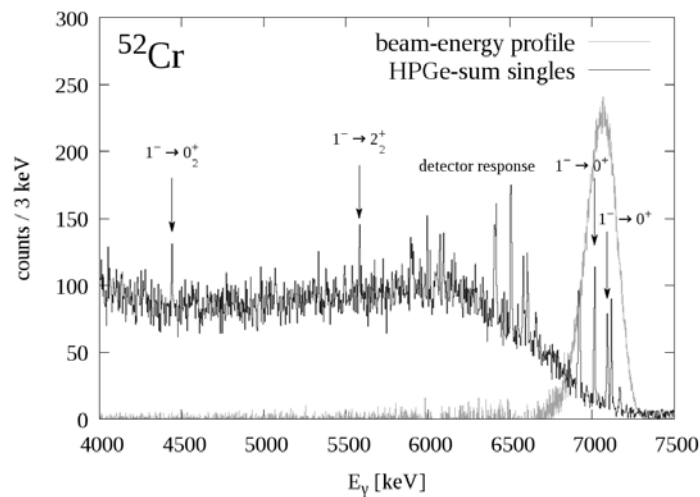


**Figure 2.** The summed spectrum of all HPGe detectors for a  $\gamma$ -ray beam energy of 7.1 MeV. Transitions to the groundstate and first excited states are clearly visible. The  $\gamma$ -ray beam energy profile (grey) has a FWHM of 260 keV.

transitions (depopulations directly to the groundstate) and inelastic transitions (depopulation to excited states) can be clearly distinguished as demonstrated in Fig. 2. The energy resolution of the highly efficient LaBr detectors is sufficient to apply gates on the depopulating  $\gamma$ -rays of the first excited states, e.g., the  $2_1^+ \rightarrow 0_1^+$  transition. Hence, several inelastic transitions to the first excited states could be observed in the gated HPGe spectra. In a previous bremsstrahlung measurement at the Darmstadt-High Intensity Photon setup (DHIPS), reduced transition strength were determined for  $^{52}\text{Cr}$ , but mainly for transitions to the groundstate only [19]. Because only dipole states within a small energy range are excited due to the quasi-

monoenergetic  $\gamma$ -ray beam, in our experiment no background from higher lying excitations decreases the sensitivity. Therefore, weaker excitations could also be investigated within this experiment. Due to this and the investigation of transitions to lower lying excited states, the total measured  $B(E1)\uparrow$  strength and  $B(M1)\uparrow$  strength up to 9.5 MeV has increased by 20% and 25%, respectively.

## 4. Discussion

### 4.1. $E1$ -strength distribution

For  $^{52}\text{Cr}$ , seven weaker  $E1$  transitions and 14  $\gamma$ -decay branching ratios to the first excited states could be observed in this experiment for the first time. Compared to the previous bremsstrahlung measurement [19], the total measured  $B(E1)\uparrow$  strength increased from  $51.2(16) \times 10^{-3} e^2\text{fm}^2$  to  $61(3) \times 10^{-3} e^2\text{fm}^2$ .

In  $^{52}\text{Cr}$  the major part of the observed  $B(E1)\uparrow$  strength is carried by four  $1^-$  states around 8 MeV (7.732 MeV, 7.896 MeV, 8.087 MeV and 8.175 MeV). With  $\sum B(E1)\uparrow = 35.5(14) \times 10^{-3} e^2\text{fm}^2$ , they contribute more than half of the total measured  $B(E1)\uparrow$  strength below 9.5 MeV. Whereas the two higher-lying  $1^-$ -states show a significant  $\gamma$ -decay branching, the excitations at 7.732 MeV and 7.896 MeV show very small  $\gamma$ -decay branchings.

### 4.2. $M1$ -strength distribution

The total  $M1$  strength from 0 to 9.5 MeV observed in the present work amounts to  $4.0(2) \mu_N^2$ . Compared to previous NRF experiments, the measured  $B(M1)\uparrow$  transition strength increased by 25% from  $3.21(13) \mu_N^2$  [19]. The additionally measured  $M1$  response results from previously unobserved states and branchings.

Shell-model calculations of  $^{52}\text{Cr}$  from Ref. [25] show the splitting into orbital and spin contributions of the  $M1$  strength for  $^{52}\text{Cr}$ . In the present experiment, for the low-lying  $1^+$  state at 6.75 MeV,  $\gamma$ -decay branchings to the  $2_1^+$  and  $0_2^+$  states were observed. This  $1^+$  state may couple to these states, which would support the character of a multiphonon  $1^+$  state that generates orbital  $M1$  strength at lower energies.

At energies around 8 MeV and 9 MeV, the  $M1$  strength is predicted to be dominated by single-particle excited states of spin-flip type. The main contribution stems from the excitation of neutron and proton  $1f_{7/2} \rightarrow 1f_{5/2}$  two-quasiparticle components. The shell-model calculations show a strong accumulation of strength at around 8 MeV for isoscalar and at around 9 MeV for isovector spin-flip  $M1$  resonances, see Ref. [25]. Comparing these theoretical results with the experimental data of the present work, the  $M1$ -strength distributions are in good agreement. The  $\gamma$ -decay branching ratios of  $1^+$  states seem to decrease with increasing energy. Two pronounced  $\gamma$ -decay branching ratios for the  $1^+$  states at 8.016 MeV and 8.583 MeV could be detected, whereas for the strong magnetic dipole excitations around 9 MeV, merely one weak branching for the  $1^+$  state at 9.212 MeV was measured.

Moreover, the  $N = 28$  isotones have different numbers of protons in the  $1f_{7/2}$  shell, which may influence strength and fragmentation of the  $M1$  strength. The strongest  $M1$  transition increases in energy with increasing number of protons along the  $N = 28$  shell closure. The excitation energies are 8.563 MeV ( $0.632(32) \mu_N^2$ ), 9.141 MeV ( $0.919(54) \mu_N^2$ ) and 10.53 MeV ( $1.262(71) \mu_N^2$ ) for  $^{50}\text{Ti}$ ,  $^{52}\text{Cr}$ , and  $^{54}\text{Fe}$ , respectively [23]. The doubly-magic nucleus  $^{48}\text{Ca}$  disagrees with this systematics, because it concentrates the  $M1$  strength with  $B(M1)\uparrow = 4.0(3) \mu_N^2$  in one single state at 10.23 MeV.

## Acknowledgments

This work was supported by the BMBF (05P2015PKEN9 and 05P15RDEN9), the DFG (ZI 510/7-1 and SFB 1245), the Alliance Program of the Helmholtz Association (HA216/EMMI),

as well as the Department of Energy, Office of Nuclear Physics under Grant No. DE-FG02-97ER41033. Julius Wilhelmy is supported by the Bonn-Cologne Graduate school.

## References

- [1] Larsen A *et al.* 2013 *Phys. Rev. Lett.* **111** 242504
- [2] Voinov A and Grimes S 2015 *Phys. Rev. C* **92** 064308
- [3] Guttormsen M *et al.* 2005 *Phys. Rev. C* **71** 044307
- [4] Larsen A *et al.* 2006 *Phys. Rev. C* **73** 064301
- [5] Larsen A *et al.* 2007 *Phys. Rev. C* **76** 044303
- [6] Voinov A *et al.* 2010 *Phys. Rev. C* **81** 024319
- [7] Larsen A *et al.* 2012 *Phys. Rev. C* **85** 014320
- [8] Buerger A *et al.* 2012 *Phys. Rev. C* **85** 064328
- [9] Larsen A *et al.* 2013 *Phys. Rev. C* **87** 014319
- [10] Wiedeking M *et al.* 2012 *Phys. Rev. Lett.* **108** 162503
- [11] Harakeh M and von der Woude A 2001 *Giant Resonances* (Oxford University Press)
- [12] Savran D, Aumann T and Zilges A 2013 *Prog. Part. Nucl. Phys.* **70** 210
- [13] Pietralla N *et al.* 2002 *Phys. Rev. Lett.* **88** 012502
- [14] Hartmann T *et al.* 2004 *Phys. Rev. Lett.* **93** 192501
- [15] Isaak J *et al.* 2011 *Phys. Rev. C* **83** 034304
- [16] Derya V *et al.* 2014 *Phys. Lett. B* **730** 288
- [17] Scheck M *et al.* 2013 *Phys. Rev. C* **87** 051304(R)
- [18] Wieland O *et al.* 2009 *Phys. Rev. Lett.* **102** 092502
- [19] Pai H *et al.* 2013 *Phys. Rev. C* **88** 054316
- [20] Heyde K, von Neumann-Cosel P and Richter A 2010 *Rev. Mod. Phys.* **82** 2365
- [21] Pai H 2016 *Phys. Rev. C* **93** 014318
- [22] Shizuma T *et al.* 2013 *Phys. Rev. C* **87** 024301
- [23] Sober D 1985 *Phys. Rev. C* **31** 2054
- [24] Scheck M *et al.* 2013 *Phys. Rev. C* **88** 044304
- [25] Langanke K *et al.* 2004 *Phys. Rev. Lett.* **93** 202501
- [26] Weller *et al.* 2009 *Prog. Part. Nucl. Phys.* **62** 257
- [27] Litvinenko V N *et al.* 1998 *Nucl. Inst. and Meth. A* **407** 8
- [28] Löher B *et al.* 2013 *Nucl. Inst. and Meth. A* **723** 136
- [29] Kneissel U, Pitz H H, Zilges A 1996 *Prog. Part. Nucl. Phys.* **37** 349